

### 3-D Experimental and FEA Investigations of Thick Single-lap Bolted Joints

Gary L. Cloud, P.E., Professor  
Mechanical Engineering Dept., Michigan State University, East Lansing, MI, 48824, USA

Florin Iancu, Research Assistant  
Mechanical Engineering Dept., Michigan State University, East Lansing, MI, 48824, USA

Xu Ding, Research Assistant  
Mechanical Engineering Dept., Michigan State University, East Lansing, MI, 48824, USA

Basavaraju B. Raju, Senior Research Engineer  
US Army Tank Automotive Command, Warren, MI, 48397, USA

#### ABSTRACT

Stresses in single-lap bolted joints of thick plates are complex and difficult to analyze. The few previous studies of stress through the thickness of bolted joints have been limited to finite element simulations and have been implemented only for the joining of relatively thin plates.

Experimental and numerical analyses were conducted to analyze the stress distribution inside thick bolted plates along the bearing plane normal to the plate surface for both composite and isotropic materials. Experimental analysis was conducted via embedded-polariscope photoelasticity, embedded resistance strain gages, and embedded fiber-optic strain sensors. The FEM analysis was performed with commercial codes using material properties and other data obtained experimentally as input. Experimental and numerical results agreed reasonably well, and are believed to depict the behavior of the joint under load well enough to facilitate improvement of joint design.

Some alternative designs were analyzed with the objective of decreasing the value of the maximum stress. The first plate presented a steel bushing around the hole, and the maximum stress in that case was decreased by 50%. The second design had the edges of the hole chamfered at a 45-degree angle. This design did not exhibit a decrease in the maximum stress, but it did show an advantageous change in the position of the maximum stress.

#### INTRODUCTION

Bolt fastening is the most widely spread method of joining because it is a non-permanent joint, it is easy to set up in a variety of conditions, it facilitates disassembly and repair, and, most of the time, it does not require manufacturing of special parts, which makes it less expensive. The problem of fastening composite materials using bolted joints is a very troublesome, because stress concentrations develop around the holes, severely reducing the strength and fatigue life of the structure. To utilize the full potential of Fiber Reinforced Polymers (FRP) in structural elements, appropriate methods for stress analysis must be developed.

Camanho and Matthews (1997) [1] summarized the previous work in predicting the failure of bolted joint composites in their review paper. The conclusion was that by taking the composite to the ultimate load, very little information could be extracted. Most of the studies on mechanically fastened joints have focused on failure tests of the structures [1, 2, 3, 4, 5, 6, 7]. Relatively few studies deal with 3-D stress analysis of bolted joints. Among the first finite element solutions created for studying contact stresses were the ones of Chen, Lee and Yeh in 1995 [8]. They were based on an incremental variational principle and the transformation matrix derived from three-dimensional contact kinematics conditions. The model took into account the effects of friction, clearance, bolt elasticity, stacking sequence and contact tractions around the bolted joint.

Another finite element analysis for laminate composite joints was developed by Barbero, Luciano, and Sacco [9]. In their paper, a contact/friction iso-parametric finite element for the analysis of connections between laminated composite plates is presented. A three-dimensional finite element model of bolted composite joints was developed by Ireman [10] to determine the non-uniform stress through the thickness of the composite laminates in

## Report Documentation Page

*Form Approved  
OMB No. 0704-0188*

Public reporting burden for the collection of information is estimated to average 1 hour per response, including the time for reviewing instructions, searching existing data sources, gathering and maintaining the data needed, and completing and reviewing the collection of information. Send comments regarding this burden estimate or any other aspect of this collection of information, including suggestions for reducing this burden, to Washington Headquarters Services, Directorate for Information Operations and Reports, 1215 Jefferson Davis Highway, Suite 1204, Arlington VA 22202-4302. Respondents should be aware that notwithstanding any other provision of law, no person shall be subject to a penalty for failing to comply with a collection of information if it does not display a currently valid OMB control number.

1. REPORT DATE <b>14 OCT 2004</b>	2. REPORT TYPE <b>Journal Article</b>	3. DATES COVERED <b>14-10-2004 to 14-10-2004</b>			
4. TITLE AND SUBTITLE <b>3-D EXPERIMENTAL AND FEA INVESTIGATIONS OF THICK SINGLE-LAP BOLTED JOINTS</b>		5a. CONTRACT NUMBER			
		5b. GRANT NUMBER			
		5c. PROGRAM ELEMENT NUMBER			
6. AUTHOR(S) <b>Raju Basavaraju; Gary Cloud; Florin Lancu; Xu Ding</b>		5d. PROJECT NUMBER			
		5e. TASK NUMBER			
		5f. WORK UNIT NUMBER			
7. PERFORMING ORGANIZATION NAME(S) AND ADDRESS(ES) <b>Michigan State University, East Lansing, MI, 48824</b>		8. PERFORMING ORGANIZATION REPORT NUMBER <b>; #14345</b>			
9. SPONSORING/MONITORING AGENCY NAME(S) AND ADDRESS(ES) <b>U.S. Army TARDEC, 6501 E.11 Mile Rd, Warren, MI, 48397-5000</b>		10. SPONSOR/MONITOR'S ACRONYM(S)			
		11. SPONSOR/MONITOR'S REPORT NUMBER(S) <b>#14345</b>			
12. DISTRIBUTION/AVAILABILITY STATEMENT <b>Approved for public release; distribution unlimited</b>					
13. SUPPLEMENTARY NOTES <b>Presented to IMAC XXIII</b>					
14. ABSTRACT <b>N/A</b>					
15. SUBJECT TERMS					
16. SECURITY CLASSIFICATION OF:			17. LIMITATION OF ABSTRACT <b>Same as Report (SAR)</b>	18. NUMBER OF PAGES <b>12</b>	19a. NAME OF RESPONSIBLE PERSON
a. REPORT <b>unclassified</b>	b. ABSTRACT <b>unclassified</b>	c. THIS PAGE <b>unclassified</b>			

the vicinity of a bolt hole. The numerical model results were compared with experimental results obtained by strain gage measurement.

Because of the complexity and difficulty of experimental stress analysis on thick single-lap bolted joints, as described above, all studies on stress analysis through the thickness of bolted joints carried out so far have been limited to finite element simulations and only for thin plate joints. Experimental results are highly desired to understand, more in detail, the real stress distribution in the through-thickness direction of bolted joints and to validate FEA studies. No published work on stress fields in thick single-lap bolted joints was found.

### RESEARCH OBJECTIVES AND APPROACHES

Thick single-lap bolted joints of epoxy and FRP plates with an aluminum plate were investigated by experiments and finite element analysis. The numerical results were correlated with those derived from experiments, which were obtained through three test methods: embedded photoelasticity, embedded resistance strain gages, and embedded fiber optic strain gages.

The methods used in this study were chosen for a number of reasons. Embedded photoelasticity has the advantage of being the only experimental method able to provide directly the values of stresses in the through-thickness direction. The disadvantage of using an embedded polariscope is that goniometric compensation methods cannot be used for fringe fraction measurements. Because of this, the results obtained by experiment have a significant uncertainty. Resistance strain gages were utilized because of their accurate response and ease of use. Fiber optic gages, among other favorable features, can be embedded in composites without seriously compromising the material.

For creating a reliable FEA model, first, a model that can be verified experimentally has to be created. Then, improvements of that model can be simulated, and qualitative as well as quantitative results can be obtained. The most difficult problem when dealing with finite element modeling of a joint resides in the necessity of creating contact surfaces. The parameters of the contact surface will greatly affect the final result. The problem becomes even more complicated when non-isotropic materials are involved. The second problem when trying to create a FEA model of the single-lap joint is simulating the clamping force that is imposed by the torque applied to the bolt and nut.

### THICK ISOTROPIC PLATE STUDY

In order to guide subsequent analysis of thick composite joints, a preliminary study of a thick joint of isotropic materials was conducted. Most of this paper deals with that problem, and, given length limitations, only minimal information about the study of thick composite plates is given.

The load cases studied are as follows: (1) pin connected - the two plates are joined by a pin and an extension force is applied on the end of one plate, while the other plate is fixed in the direction of the extension; (2) the pin was replaced by a bolt and the joint was studied for several magnitudes of torque applied to the bolt-nut pair including finger tightening (approx. 3 in-lbs of torque), 25 in-lbs torque and 40 in-lbs torque.

### EXPERIMENTAL METHODS

Two methods were implemented for the isotropic plate study: embedded polariscope photoelasticity was used to determine the shear stress distribution in the bearing plane, and resistance strain gages were employed for measuring strain in the same plane.

#### 1. Fabrication of specimen.

The polarizer, the analyzer and the quarter wave plates were embedded into the specimen, as shown in Figure 1. The polarizer and the retarding film were cut from commercially available sheet of Polaroid filter medium, type CP -01P

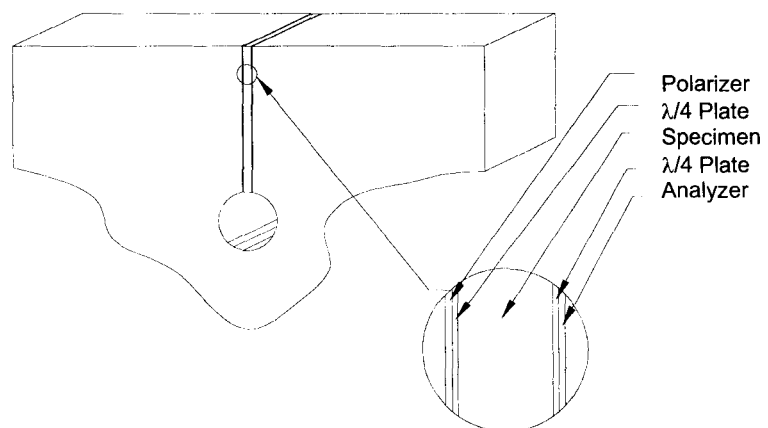


Figure 1. Embedded polariscope in a birefringent plate.

(made by International Polarizer, Inc.). The quarter wave plates have the role of converting the linear polarized light emerging from the polarizer into circularly polarized light. The circular polarization eliminates isoclinics (loci of points of constant inclination of the principal axes of refraction)

A 4 by 8 inch piece was cut out from a commercial photoelastic sheet (PSM-9), manufactured by Photoelastic Division of Measurements Group, Inc. The material has the following mechanical properties:  $E = 4.78 \text{ e5psi}$ ,  $\nu = 0.38$ . A hole of 15/32 inches in diameter was drilled at 1.5 inches from the short side and 2 inches from the long side as in Figure 2. From the hole to the short side, a 0.185 inches slice or slat was removed. Three strain gages were attached to the slice as in Figure 3.

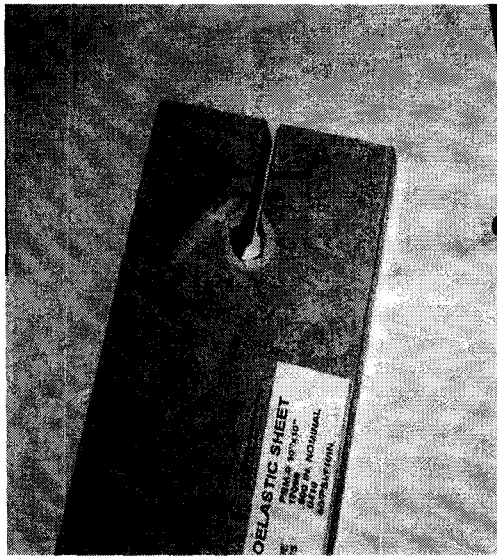


Figure 2. Initial stage in the construction of the specimen.

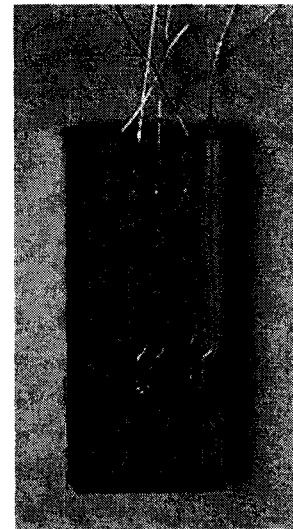
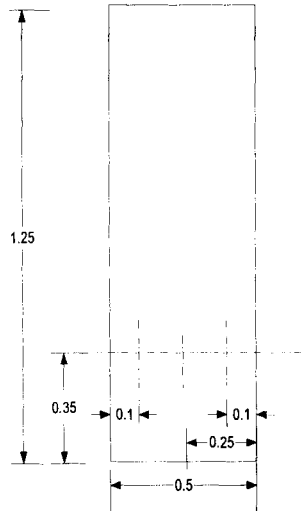


Figure 3. Strain gages attached to the removed slice

Next, a polarizer and retarder plates were glued on both sides of the slice to form a light field polariscope. After all these operations, the slice was glued back into its original place inside the plate and the bolt hole was reamed to 0.5 inches as shown in Figure 4.

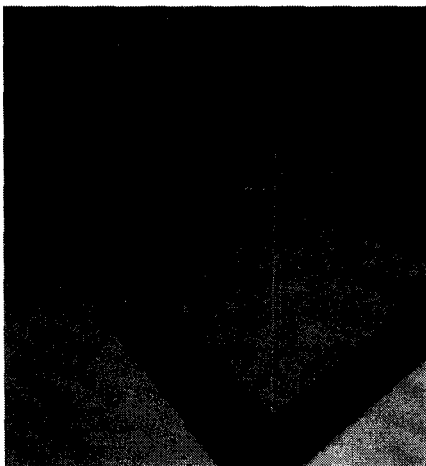


Figure 4. The final form of the specimen.

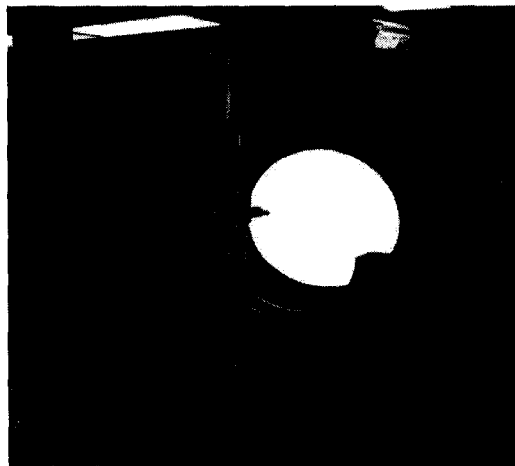


Figure 5. Loading frame.

## 2. Loading conditions

The loading frame can be seen in Figure 5. Both plates are 8 x 4 x .5 inches. The supporting plate is made of aluminum, 2024-T4, with the following material properties:  $E = 1.01e7\text{psi}$ ,  $\nu = 0.34$ . During tests, photoelasticity fringe patterns were recorded by a COHU CCD camera and the strain readings from strain gages were obtained by commercial strain indicators.

### FINITE ELEMENT ANALYSIS

The numerical study of the single lap joint was done using the explicit finite element code ABAQUS 6.2 [11]. The preprocessor used to build the finite element model was HyperMesh 5.0 [12], and the postprocessor used to view the results was ABAQUS/Viewer 6.3-1. Several finite element models were created in order to study the two types of joints: pin connected and bolt connected. A typical mesh of the bolt connected joint is shown in Figure 6.

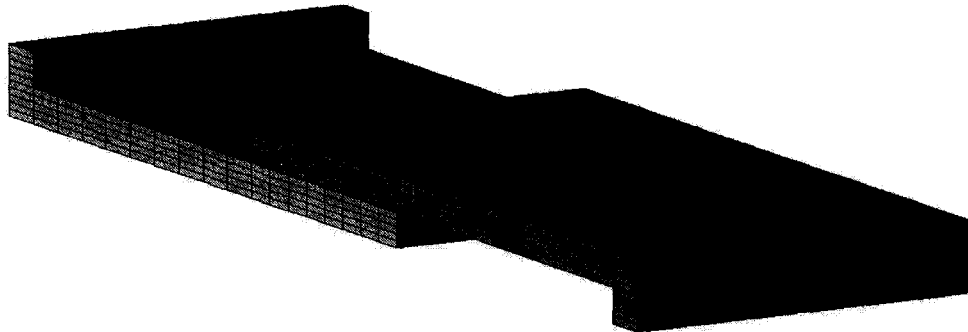


Figure 6. Typical mesh of a single lap bolted joint of two plates.

The mesh is divided into two regions: a square corresponding to the overlap area with a finer mesh surrounding the bolt hole and a rectangle with a coarser mesh. The plates have an offset part at the ends so the loading conditions can be uniaxial. The square is in turn divided into two sub-parts: a cylindrical part under the washers and the rest of the square. Thirty-two elements were used around the hole. The same number of elements was used to model the circumference of the bolt and bolt head. All the elements used for modeling the geometry were C3D8I, eight-node, solid elements.

The bolt, bolt head and washer were modeled as a single object to limit the number of contact surfaces in the model. The nut was modeled together with the second washer and a contact pair was created between the inside of the washer and the outside of the bolt. A high friction coefficient was applied to these surfaces, in order to simulate the effect of the thread. Figure 7 shows the nut-washer component and the whole fastening assembly. The model was based on idealization of the fastening system [13]. The torque applied to the bolt and nut was converted into a compressive load applied to the bolt-head and nut (see Figure 8).

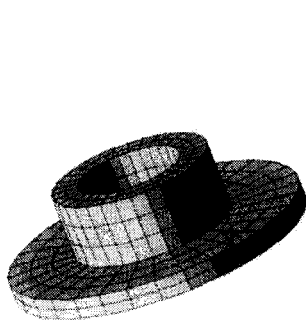


Figure 7. FEA mesh of the nut-washer unit and the fastening units.

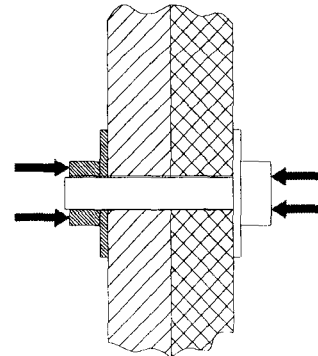
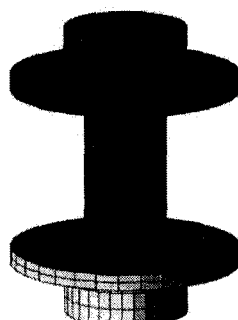


Figure 8. Fastening forces on the joint.

Contacts between the aluminum and epoxy, the aluminum and the steel bolt-washer, the plates and the bolt, and the epoxy and nut-washer were modeled using the contact pair approach in ABAQUS. This approach is based on

the master-slave concept, and the contact problem was solved using the Lagrange multiplier method. Since sliding between parts was expected to be small, the "small sliding" option was used in all analyses. This option implied that possible contact between master and slave nodes is defined at the beginning of the analysis and is not redefined during the analysis. The contact surfaces used in the model are shown in Figure 9. Two different surface interaction properties were created for applying two friction coefficients to the contact pairs.

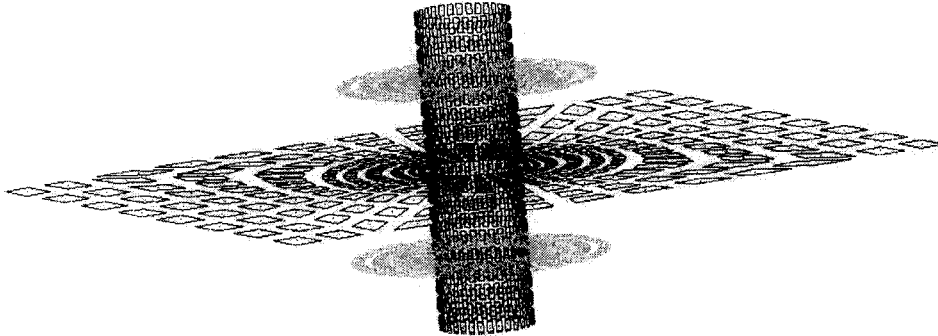


Figure 9. Contact pairs involved in a single lap bolted joint.

The epoxy plate was fixed for one direction at one end. The clamping force was simulated by a distributed nodal load applied on the bolt head and nut in every point of their volume. On the nodes of the end of the aluminum plate, a static force was applied as a distributed load.

## RESULTS AND REMARKS FOR ISOTROPIC PLATE

Experimental and numerical results were compared by case.

### 1. Pin connection

In the first studied case the two plates were connected by a half inch diameter pin. The joint was loaded progressively up to 50lbs. Besides the fringe pattern recorded by the camera, some strain measurement were recorded from inside the tested plate.

The photoelasticity investigation delivered the following result for 50lbs loading on the joint (Figure 10). It can be seen that in the lower left corner, which is the point closest to the aluminum plate during loading, and which has the highest shear stress, there are 3.5 fringes (the white lines are full order fringes and the black ones are half order fringes). The maximum shear stress is determined as 700 psi.

Figure 11 presents the FEA distribution of the shear stress in the bearing plane (the same as embedded polariscope) and Figure 12 is the distribution of the normal strain in the 2 direction, for 50 lbs load. As can be seen, the map of the shear stress obtained numerically matches the stress distribution pattern obtained by photoelasticity.

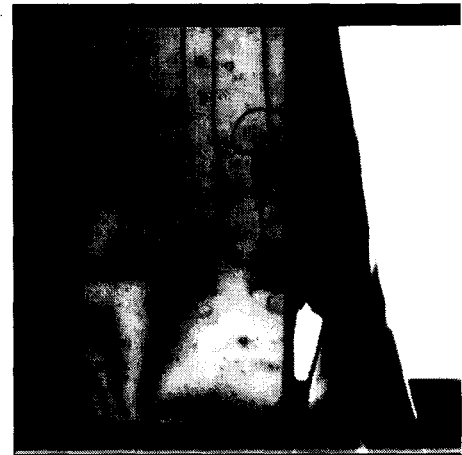


Figure 10. Shear stress fringe pattern for a pin connection loaded at 50lbs.

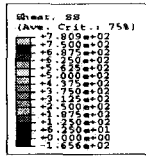


Figure 11. Distribution of shear stresses in the bearing plane of the epoxy plate for pin connection and 50 lbs load on the joint (results are in psi).

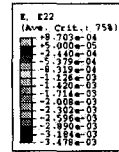


Figure 12. Distribution of normal strain in 2-direction in the bearing plane of the epoxy plate for pin connection and 50 lbs load on the joint (results are in  $\mu\epsilon$ ).

Strain results that were recorded by the strain gages placed in points A, B and C (Figure 13) for different loads as well as shear stress at points D, E, and F from the photoelasticity test are compared in Figures 14 and 15 respectively.

The photoelasticity method used for this experiment, the embedded polariscope, has one major disadvantage. Optical compensation methods cannot be applied in order to obtain an exact value. That is why all the values on the graph have a  $\pm 50$ psi error bar.

As can be seen from Figure 15, the numerical results match very closely the experimental ones at points B and C. In point A, the experiment is providing results with higher magnitudes than FEA. Since point A is the closest to the aluminum plate, the cause of the error could be the friction between the two plates, friction that was not accounted for in the numerical model. The maximum stress on the bearing plane is where the epoxy plate meets the aluminum plate and the pin.

This is the predicted result since the two plates are moving with respect to each other, movement which causes the tilting of the pin. The new position of the pin changes its contact with the plate to a small area. By applying a constraint in the movement of the pin, a decrease in the value of the maximum stress is expected. This constraint can be achieved by replacing the pin with a bolt and applying a torque on the bolt and nut.

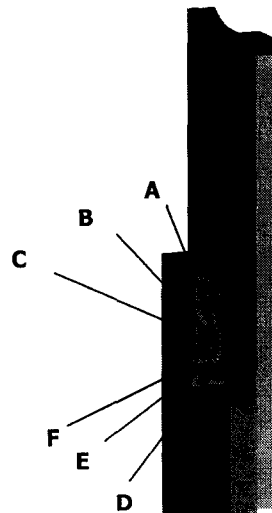


Figure 13. Position of the six measuring points.

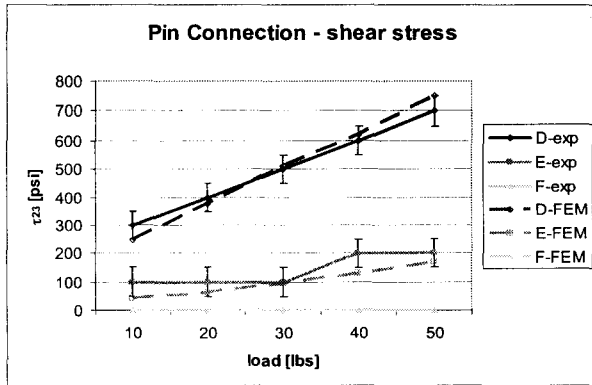


Figure 14. Shear stress in the bearing plane versus the load applied to the joint (pin connected joint).

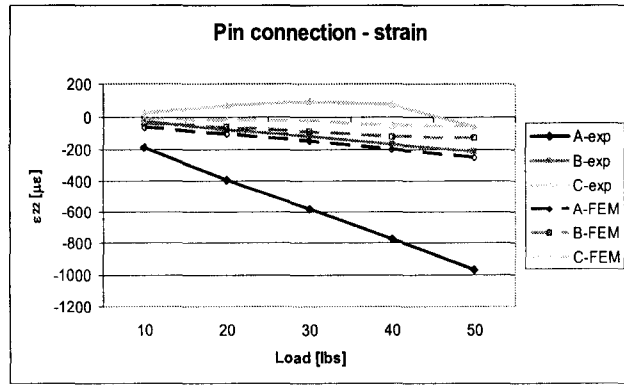


Figure 15. Normal strain in the bearing plane versus the load applied to the joint (pin connected joint).

## 2. Bolt connection

The pin was replaced by a bolt, on which a torque of about 4 in-lbs was applied, equivalent to finger tightening. The joint was loaded from 0 lbs to 120 lbs. For the maximum load, the shear stress distribution looks like in Figure 16. In Figures 17 and 18, the shear stress results obtained by FEA for 120 lbs load and normal strain for 140 lbs load are presented.

There are no high concentrations of stresses. The distribution is almost uniform. In the left corner there is only one fringe, while on the rest of the lower edge half of a fringe is visible. This means that the highest shear stress is in the same corner as for pin connection; but, for a much higher load, the stress is only about 200 psi. The torque reduces the stress concentration, as expected. Figures 19 and 20 indicate the comparison between test and FEA results.

The difference in stress values obtained by FEA and photoelasticity investigations is under 15%. That is a reasonable result, taking into consideration that the photoelasticity provides results with a margin of error of 50 psi. As for the pin connection, the strain results are not that close, especially for strain gage number one. The values obtained numerically and experimentally are close for small loads, up to 70 lbs.



Figure 16. Shear stress fringe pattern for a bolt connection loaded at 50lbs with a finger tighten.

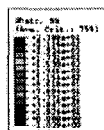


Figure 17. Distribution of shear stresses in the bearing plane of the epoxy plate for 4 in lbs torque on the bolt and 120 lbs load on the joint (results are in psi).

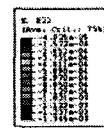


Figure 18. Distribution of normal strain in 2-direction in the bearing plane of the epoxy plate for 4 in lbs torque on the bolt and 140 lbs load on the joint (results are in  $\mu\epsilon$ ).

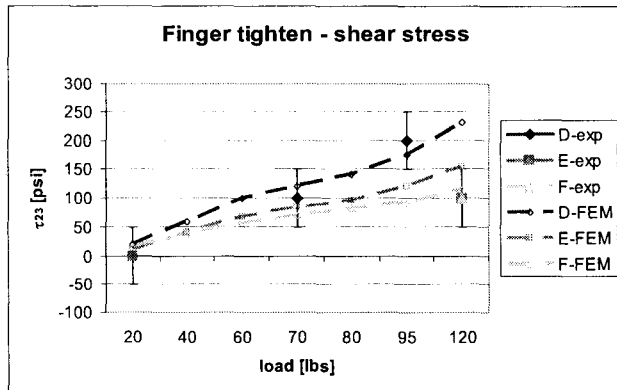


Figure 19. Shear stress in the bearing plane versus the load applied to the joint (bolt connected joint with 4 in lbs torque).

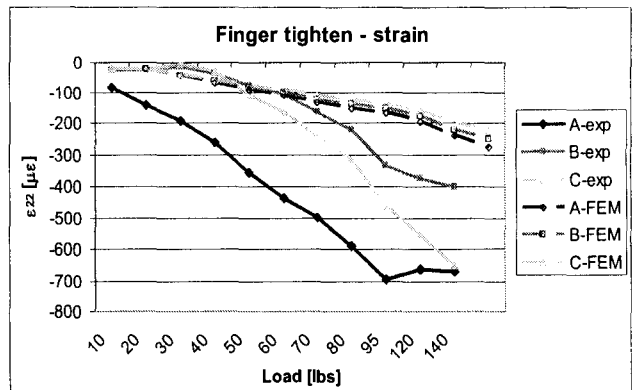


Figure 20. Normal strain in the bearing plane versus the load applied to the joint (bolt connected joint with 4 in lbs torque).

From Figures 10 and 16, two conclusions can be drawn. The magnitudes of stresses are much lower for a bolt connection than for pin connection. Also, the bolt, even with low clamping, is held straighter by the head and washers. That means friction between the two plates is taking over some of the load in the joint. The second conclusion is that the fringe pattern has changed, the stress being more uniformly distributed over the thickness of the plate, which was the desired result.

The bolt was tightened to two different torque levels: 25 in lbs, which was converted to normal loading on the bolt head and nut of 190 lbs. The second torque was 40 in lbs, which was converted to 300 lbs. In Figures 21 and 22, a comparison between the FEA results and the experimental ones is presented for the bolt connection with a torque of 25 in-lbs applied on the bolt. Figure 21 displays the results of the shear stress in the bearing plane, while Figure 22 shows strain values in the same plane.

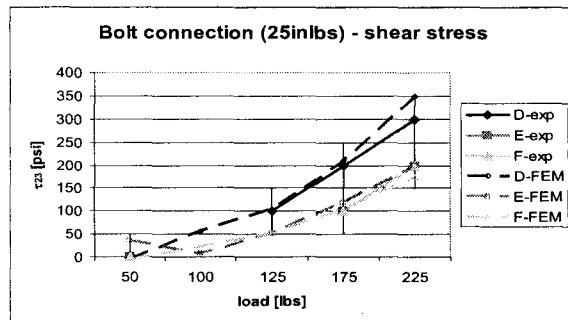


Figure 21. Shear stress in the bearing plane versus the load applied to the joint (bolt connected joint with 25 in-lbs torque).

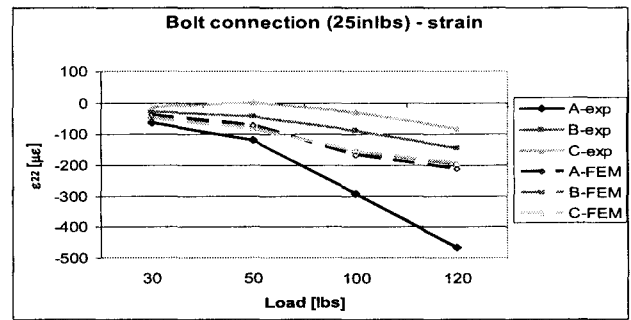


Figure 22. Normal strain in the bearing plane versus the load applied to the joint (bolt connected joint with 25 in-lbs torque).

The shear stresses have very similar values for experimental and numerical results at all three points measured. For the point of maximum stress, FEA predicts a higher value than the experiment, which could lead to a safety factor in the design of the product.

The strain results provided by experiment and finite element modeling appear to be similar for the middle point only. The causes of errors have both experimental and numerical provenance: delamination of the investigated slice from the plate, which causes false readings from the strain gages, presence of an air bubble next to the third strain gage, and application of the force on the bolt on the same direction through all the steps of the simulation.

The same comparisons as for 25 in-lbs torque are displayed in Figures 23 and 24 but for 40 in-lbs torque. As can be seen the same remarks as for 25 in-lbs torque can be made (see Figures 21 and 22), which leads to the conclusion that the numerical model provides consistent results.

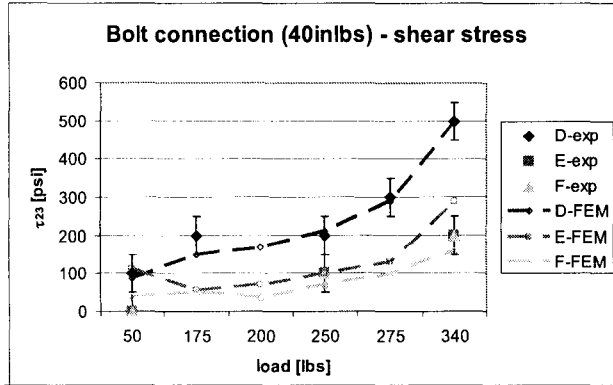


Figure 23. Shear stress in the bearing plane versus the load applied to the joint (bolt connected joint with 40 in-lbs torque).

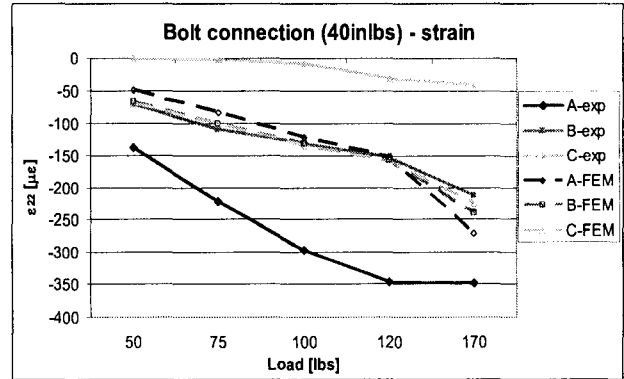


Figure 24. Normal strain in the bearing plane versus the load applied to the joint (bolt connected joint with 40 in lbs torque).

### 3. Numerical alternative designs for decreasing the maximum stress

To decrease the stresses in bolted plates, two alternative designs were proposed and analyzed numerically. The first design includes a steel bushing around the hole in the plate. A section of the mesh of the plate can be seen in Figure 25. The thickness of the bushing is 0.05 inches and the material has the following properties:  $E = 30e6$  psi and  $\nu = 0.28$ . The role of the bushing is to take over the high stress concentration zone. Also, the steel bushing makes the plate stiffer in the longitudinal direction, and especially in the bearing zone.

The distribution of the shear stress in the bearing plane for this alternative design can be seen in Figure 26. This load case incorporates 4 in-lbs torque on the bolt and 120 lbs loading of the joint. As can be seen a maximum stress of only 105 psi is developed inside the epoxy plate, while for a regular plate, the stress is 230 psi. This design decreases the maximum stress in the bearing plane of the epoxy plate by 50 %.

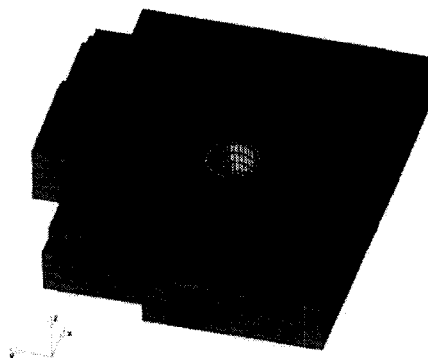


Figure 25. Typical mesh of the plate with a steel bushing around the hole.

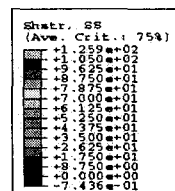


Figure 26. Distribution of shear stresses in the bearing plane of the modified epoxy plate for 4 in lbs torque on the bolt and 120 lbs load on the joint (results are in psi).

The second model exhibits a 45-degree chamfer of the edge of the hole. A portion of the mesh of this alternative design plate can be seen in Figure 27. For this second design the results can be seen in Figure 28. Although the value of the maximum stress has not been lowered, its position has changed. Now, the maximum stress is in the middle of the bearing section, possibly reducing the risk of cracking or, in the laminated composite materials, of delamination.

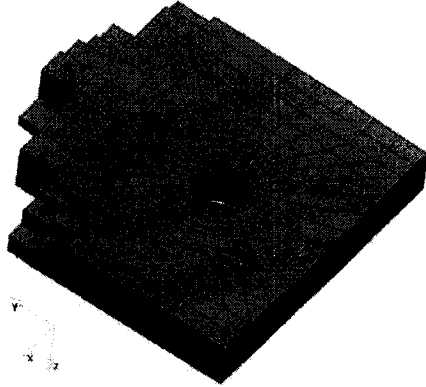


Figure 27. Typical mesh of the plate with a trim of the edge of the hole.

Stat. SS	(Ave. Crit.: 75%)
MIN	+1.257e+03
MAX	-2.500e+02
Avg	-2.077e+02
StDev	-1.653e+02
StErr	+1.230e+02
StErr	-8.060e+01
StErr	+3.825e+01
StErr	-4.036e+00
StErr	+4.644e+01
StErr	-8.879e+01
StErr	-1.311e+02
StErr	-1.735e+02
StErr	-2.158e+02
StErr	-2.582e+02

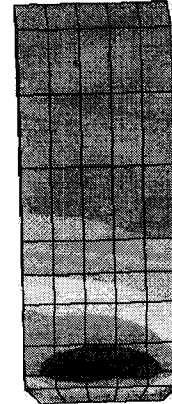


Figure 28. Distribution of shear stresses in the bearing plane of the modified epoxy plate for 4 in lbs torque on the bolt and 120 lbs load on the joint (results are in psi).

### THICK COMPOSITE JOINT

Investigation of thick composite joints by embedded photoelasticity has proven not entirely feasible for reasons that cannot be expounded within the confines of this paper. Attention focused on alternate methods for obtaining the needed 3-D information, including, for example, embedded grating moire. Fiber optic strain gages were chosen because they can be embedded in the specimen without unduly compromising the local properties of the FRP, they have appropriate range and sensitivity, the similarity problem is solved, and they offer a possible technique for long-term health monitoring of structures. Cost, fragility, and the fact that the data are pointwise are the primary disadvantages.

Three brands of gages were given preliminary study, and the ones made by FISO Ltd. (Montreal, Canada) were chosen for this research. These sensors are of the Fabry-Perot interferometer type. Several sensors and the matching signal conditioner and readout instrument were obtained.

As a preliminary test, only one fiber optic sensor was embedded into a composite specimen as it was being laid up by hand. A plain weave E-glass fabric style 3733 with S-910 finish manufactured by J.P. Stevens was chosen as the reinforcement. The resin 20-3302 made by the Epoxies, Etc... was used as the matrix material. Specimen geometry was similar to that shown earlier in this report. A photograph of the finished specimen is shown in Figure 29.

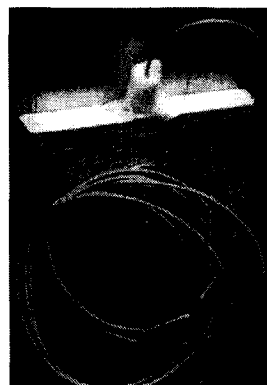


Figure 30. Preliminary composite joint specimen with one embedded fiber optic strain gage.

This specimen was tested according to the protocol outlined for the isotropic specimen. Some typical results for the finger-tightened case and for the 40 in-lb tightening torque case are shown in Figures 30 and 31. The effects of the clamping force in increasing hysteresis of the joint are apparent.

**DISCUSSION OF RESULTS AND CONCLUSIONS**

In this study, several experimental and numerical analyses were conducted to evaluate the behavior of thick single-lap bolted joints involving both isotropic and composite plates. The main interest of this analysis was the stress inside the plate along the bearing plane.

For the isotropic plate, experimental analysis was conducted via photoelastic investigations, by creating an embedded polariscope in the bearing plane of the plate. Additionally, resistance strain gages were mounted inside the plate along the same plane. The numerical modeling was performed with the Abaqus commercial code using material properties and other data obtained experimentally as input. The results were able to explain the behavior of the joint when loaded.

The maximum shear stress in the bearing plane of the photoelastic plate caused by the loading of the joint was created largely by tilting of the bolt. It has been proven that the higher the torque applied on the bolt, the lower the maximum stress in the plate. Yet, if a certain value of this torque is exceeded, failure of the joint will occur. Even a small value of torque, equivalent with finger tightening the bolt, will decrease the maximum shear stress by more than 50%.

Having confidence in the numerical model created, two other plates were designed in order to decrease the value of the maximum stress. The first plate incorporated a steel bushing around the hole, and the value of the stress in the photoelastic plate was diminished by 50%. The second design presented had the edges of the hole chamfered at a 45 degrees angle. This design didn't show a decrease in the maximum stress, but it showed a change in the position of the maximum stress, to a location less susceptible to cracking or delamination (in the case of laminated composite materials). Taking into consideration that the second design is just a little or no more costly than the original design, it seems to be a good alternative for improving the bolt joining of composite plates, but additional research is needed to prove this contention.

Tests thus far with embedded fiber optic strain gages confirm that this approach is viable for gaining experimental knowledge of the strain field at many points inside a thick composite plate. The properties of the composite material have been measured using these sensors, and a specimen with an internal array is being tested.

**REFERENCES**

1. Camanho, P. P. and Matthews, F. L., "Stress analysis and strength prediction of mechanically fastened joints in FRP: a review," *Composites Part A*, 529-547, (1996).
2. Dano, M. L., Gendron, G., et al., "Stress and failure analysis of mechanically fastened joints in composite laminates," *Composite Structures*, 50, 287-296, (2000).

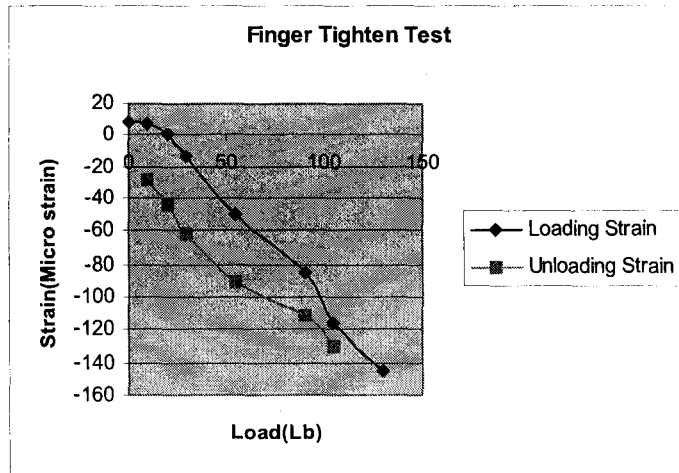


Figure 30. Composite internal strain from FOSG for finger-tightened joint

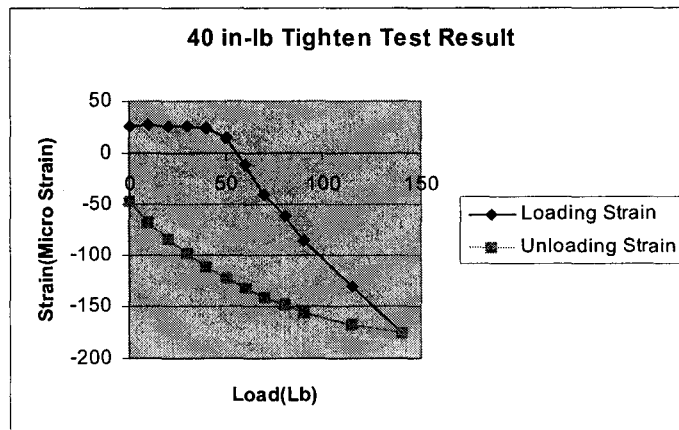


Figure 31. Composite internal strain from FOSG for joint tightened to 40 in-lb

3. Ireman, T., Ranvik, T., et al., "On damage development in mechanically fastened composite laminates," *Composite Structures*, 49, 151-171, (2000).
4. McCarthy, M. A., Lawlor, V. P., et al., "Bolt-hole clearance effects and strength criteria in single-bolt, single-lap, composite joints," *Composite Science and Technology*, 62, 1415-1431, (2002).
5. Park, H. J., "Effects of stacking sequence and clamping force on the bearing strengths of mechanically fastened joints in composite laminates," *Composite Structures*, 53, 213-221, (2001).
6. Starikov, R. and Schon, J., "Quasi-static behaviour of composite joints with protruding-head bolts," *Composite Structures*, 51, 411-425, (2001).
7. Zetterberg, T., Astrom, B. T., et al., "On design of joints between composite profiles for bridge deck applications," *Composite Structures*, 51, 83-91, (2001).
8. Chen, W. H., Lee, S. S. et al., "Three-dimensional contact stress analysis of a composite laminate with bolted joint," *Composite Structures*, 30, 287-297, (1995).
9. Barbero, E. J., Luciano, R., et al., "Three-dimensional plate and contact/friction elements for laminated composite joints," *Computer and Structures*, 54(4), 689-703, (1995).
10. Ireman, T., "Three-dimensional stress analysis of bolted single-lap composite joints," *Composite Structures*, 43, 195-216, (1998).
11. ABAQUS/Standard user manual ver. 6.2. Hibbitt, Karlsson & Sorensen, Inc., (1998).
12. HyperMesh user manual ver. 5.0, Altair Computing, Inc., (2001).
13. Speck, J. A., *Mechanical fastening, joining and assembly*, Marcel Dekker, Inc., (1997).